Atomic-resolution study of lattice distortions of buried $In_xGa_{1-x}As$ monolayers in GaAs(001)

T.-L. Lee and M. R. Pillai
Department of Materials Science and Engineering and Materials Research Center, Northwestern University, Evanston, Illinois 60208

J. C. Woicik
National Institute of Standards and Technology, Gaithersburg, Maryland 20899

G. Labanda, P. F. Lyman, and S. A. Barnett
Department of Materials Science and Engineering and Materials Research Center, Northwestern University, Evanston, Illinois 60208

M. J. Bedzyk
Department of Materials Science and Engineering and Materials Research Center, Northwestern University, Evanston, Illinois 60208 and Materials Science Division, Argonne National Laboratory, Argonne, Illinois 60439

(Received 24 June 1999)

X-ray standing wave measurements were used to study the strain in one monolayer of pseudobinary alloy $In_xGa_{1-x}As$ buried in GaAs(001) by molecular-beam epitaxy. The measured In position along the [001] direction exhibited a nearly linear dependence on the In concentration *x*, thus supporting the validity of macroscopic continuum elasticity theory at the one-monolayer limit. A random-cluster calculation using a valence force field was performed to explain microscopically the origin of the vertical expansion of the strained monolayer observed by the experiment. The calculated As-In-As bond angle and the positions of the first-nearest-neighbor As atoms of In suggest that the nearly linear dependence of the In height on the alloy composition is a combined result of the As-In-As bond bending and the local lattice distortion at the GaAs/$In_xGa_{1-x}As$ interface. The calculated In-As and Ga-As bond lengths were found to depend weakly on the In concentration, consistent with an earlier calculation for the case of a thick $In_xGa_{1-x}As$ film on GaAs(001) and the available x-ray absorption fine-structure data. [S0163-1829(99)05143-7]

Highly strained III-V semiconductor heterostructures, e.g., $In_xGa_{1-x}As$/GaAs, have been widely investigated and used in devices such as high-speed transistors and quantum well lasers.[1] Recent studies of monolayer-period strained III-V superlattices have demonstrated great potential in forming a type of nanostructure with enhanced optical properties.[2,3] In predicting electronic and optical properties, continuum elasticity theory is used to evaluate the strain state.[4] In a planar pseudomorphically grown heterostructure, the film is constrained to have the same in-plane lattice parameters as the substrate, while it is free to relax in the growth direction. This results in a distortion of the unit cell of the film. Based on macroscopic continuum elasticity theory, for cubic materials with the film parallel to the (001) plane, the strain normal to the (001) plane ($\epsilon_\perp$) is related to the in-plane strain ($\epsilon_\parallel$) by

$$\epsilon_\perp = -2\frac{C_{12}}{C_{11}}\epsilon_\parallel, \tag{1}$$

where C_{ij} are the bulk elastic constants for the embedded material. For InAs/GaAs, these constants are $C_{11} = 8.329\times10^{11}$ and $C_{12} = 4.526\times10^{11}$ dynes/cm^2 for InAs,[5] and the lattice misfit between InAs and GaAs leads to $\epsilon_\parallel = -6.7\%$. Thus, Eq. (1) predicts a strain of $\epsilon_\perp = 7.3\%$ for a pseudomorphic InAs layer buried in GaAs(001). Experimental evidence from Brandt *et al.*,[6] based on a high-resolution electron microscopy analysis, showed good agreement with Eq. (1) for a three-monolayer (ML) InAs sample, but gave a much larger $\epsilon_\perp$(12.46%) for a sample with 1 ML of InAs. This discrepancy has drawn attention to the issue of whether macroscopic elasticity theory can correctly describe the strain in an ultrathin film.[7–10]

In the present paper, we perform an x-ray standing wave (XSW) study to directly measure the strain in one ML of $In_xGa_{1-x}As$ buried in GaAs(001) by precisely locating the indium position relative to the underlying GaAs substrate unit cell. These results are shown to agree favorably with the macroscopic continuum elasticity theory. In addition, we carry out a random-cluster calculation for a buried ML using the Keating valence-force field to understand the local structural variations in the thin heterolayers. This calculation provides us with more insight into the microscopic behavior of strain in ML-thick films.

The films were grown by conventional molecular-beam epitaxy (MBE) on semi-insulating polished GaAs substrates cut within 0.5° of the (001) plane. The substrates were cleaned with acetone and methanol and mounted using indium on a silicon block that served as a resistive heating element. They were then inserted into the MBE chamber and annealed for 10 min at a substrate temperature $T_s = 570\,^\circ$C in a 1.5×10^{-5} torr As_4 overpressure. *In situ* substrate cleaning was carried out with 1 keV Ar ions impinging at 15° from the surface in the [001] direction up to a dose of 2.3×10^{16} ions-cm^{-2} sec^{-1} at the same T_s and As_4 ambient. These bombardment conditions for as-prepared GaAs substrates have been shown to yield smooth, essentially defect-free GaAs surfaces.[12] A 2-μm GaAs buffer layer was first

grown on the sputter-cleaned GaAs surface at $T_s = 570\,^{\circ}\mathrm{C}$. During the last 1000 Å of the buffer-layer growth, T_s was ramped down to 500 °C. One ML of $In_xGa_{1-x}As$ was then deposited at 500 °C followed by a 100 Å-thick GaAs capping layer grown at the same T_s. Three samples with different In concentrations were prepared for the XSW measurements.

The chemical composition of each buried layer was measured by fluorescence yield analysis using an In-implanted Si crystal with a concentration calibrated by Rutherford backscattering as the standard. By comparing the fluorescence yields of the samples to those of the standard, the absolute In coverages of samples *A*, *B*, and *C* were determined to be 0.4, 0.6, and 1.1 ML, respectively, with an estimated error of 0.1 ML. By applying Eq. (1), and assuming Vegard's law, the macroscopic elasticity theory predicts the perpendicular strains within the $In_xGa_{1-x}As$ layers of sample *A*, *B*, and *C* to be 2.7%, 4.1%, and 7.3%, respectively.

The XSW experiments were performed at beamline X15A of the National Synchrotron Light Source (NSLS).[13] The measurement consists of simultaneously recording the fluorescence spectra and the reflectivity from a sample while scanning a double-crystal Si(004) monochromator in energy through the (004) Bragg reflection of the GaAs substrate.[14] This scan causes the standing wave to phase shift inward by one half of a *d* spacing relative to the *hkl* diffraction planes, and induces a characteristic modulation of the fluorescence yield. The samples were kept in a helium atmosphere throughout the x-ray measurements in order to eliminate Ar $K\alpha$ from the fluorescence spectrum and to reduce the attenuation of the low-energy fluorescent x-rays.

Based on von Laue and Ewald's dynamical diffraction theory,[15] this fluorescence modulation, $Y(\theta)$, for atoms at or near the surface, can be described as:

$$Y(\theta) = Y_{\mathrm{OB}}\{1 + R(\theta) + 2\sqrt{R(\theta)}f_{\mathbf{H}}\cos[\nu(\theta) - 2\pi P_{\mathbf{H}}]\}, \tag{2}$$

where Y_{OB} is the off-Bragg fluorescence yield, $R(\theta)$ is the reflectivity and $\nu(\theta)$ is the phase difference between the incident and the reflected plane waves. The quantities $f_{\mathbf{H}}$ and $P_{\mathbf{H}}$ in the last term, which are referred to as the coherent fraction and the coherent position, correspond to the amplitude and phase, respectively, of the **H**th Fourier component of the spatial distribution of the fluorescence-selected atom. More specifically, the coherent fraction can be expressed as a product of three factors[16]

$$f_{\mathbf{H}} = C a_{\mathbf{H}} D_{\mathbf{H}}, \tag{3}$$

where *C* is the ordered fraction, $a_{\mathbf{H}}$ is the geometrical factor, and $D_{\mathbf{H}}$ is the Debye-Waller factor.

Figure 1 shows the In *L* fluorescence yields as a function of the incident angle θ for samples *A*, *B*, and *C* along with the (004) reflectivity *R*. The parameters of the XSW analysis, determined by the best fits of Eq. (2) to our data, are summarized in Table I. For samples *A* and *B*, if one assumes that the In occupies only one lattice position when projected along the [004] axis, i.e., $a_{004} = 1$ in Eq. (3), the In coherent fraction f_{004} should be close to the room-temperature GaAs(004) Debye-Waller factor $D_{004} = 0.86$.[17] The present measured coherent fractions for *A* and *B*, when compared with D_{004}, can be interpreted to mean that 91% ($C = 0.91$)

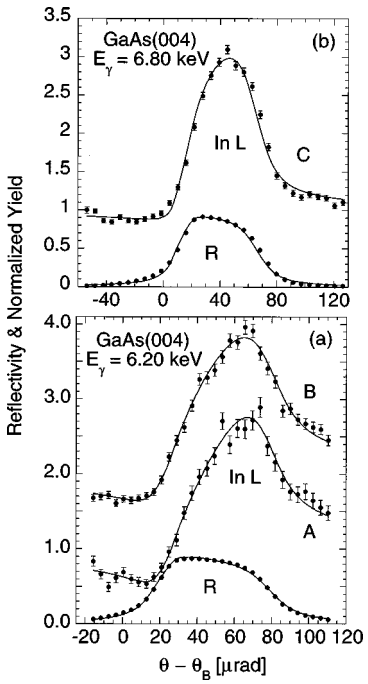

FIG. 1. The (004) XSW data and the theory (solid lines) for the normalized In *L* fluorescence yields and the GaAs(004) reflectivity *R* versus incident angle θ for (a) samples *A* and *B* and (b) samples *C* (see text). The In *L* curve for sample *B* is offset by 1 for the purpose of clarity.

of the In atoms are located at the ordered positions defined by their P_{004}, and the remaining 9% are randomly distributed. The high measured values of f_{004} indicate that under the specified growth condition a buried heterostructure with 1-ML $In_xGa_{1-x}As$ well confined in a single layer has been achieved.

The In coherent positions determined in Fig. 1 are $P_{004} = 1.05 \pm 0.01$ for sample *A* and $P_{004} = 1.08 \pm 0.01$ for sample *B*, which locate the heights of the In to be 1.48 ± 0.01 Å and 1.53 ± 0.01 Å, respectively, above the nearest-As plane extrapolated from the substrate (Fig. 2). Based on Vegard's law, the (004) *d* spacing of cubic $In_xGa_{1-x}As$ is 1.454 Å for $x = 0.4$ and 1.474 Å for $x = 0.6$. Therefore, our measurements have detected a vertical expansion of the buried layer due to the lateral compression. The elastic deformation of a unit cell can be, in general, described macroscopically by the continuum elasticity theory. However, when applying the same theory to a one ML-thick strained film, certain issues must be considered more carefully. First, strain is a relative quantity; therefore, the placement of the boundary of the strain-effected region is more critical for the case of a buried single monolayer. Second, within the strained region, the lattice deformation must be uniform to allow the strain calculated in Eq. (1) to be used for predicting the position of an atom in the strained layer. For an (001)-oriented film of zinc-blende structure, this uniformity is ensured by the fact that the four different directions along the tetrahedral bonds are all equivalent with respect to the in-plane stress imposed by the substrate. If we assume that the boundary of the strained region is at the nearest As planes above and below the In_xGa_{1-x} layer, the indium (004) coherent position can be related to the vertical strain $\epsilon_\perp$ by

TABLE I. Results of the (004) XSW measurements. The coherent fractions f_{004} and coherent positions P_{004} were determined by χ^2 fit of Eq. (2) to the data. The theoretical values of $\epsilon_\perp$ and P_{004} were obtained by applying Eq. (1) and Eq. (4) for *A* and *B*, respectively, using calibrated *x* values. The $\epsilon_\perp$ of *C* was calculated for 1 ML of buried InAs. The theoretical P_{004} was derived from the (004) Fourier component of 1.1 ML of strained InAs (see text).

Sample	Thickness (ML)	$x(\mathrm{In}_x\mathrm{Ga}_{1-x}\mathrm{As})$	f_{004}	P_{004}	$\epsilon_\perp$ theory	P_{004} theory
A	1	0.4	0.79 ± 0.02	1.05 ± 0.01	2.7%	1.056
B	1	0.6	0.77 ± 0.02	1.08 ± 0.01	4.1	1.086
C	1.1	1.0	0.67 ± 0.02	1.165 ± 0.01	7.3%	1.165

$$P_{004}=(1+\epsilon_\perp)a_{f0}/a_{s0}, \tag{4}$$

where $a_{s0}=5.6532$ Å is the GaAs substrate lattice constant, and a_{f0} is the unstrained bulk lattice constant for the $\mathrm{In}_x\mathrm{Ga}_{1-x}\mathrm{As}$ layer. Therefore, macroscopic continuum elasticity theory [Eq. (1)] predicts, through Eq. (4) and Vegard's law, that the In height P_{004} increases in a nearly linear manner from 0 to 0.15 as *x* varies from 0 to 1. In particular, Eq. (4) predicts that $P_{004}=1.056$ for sample *A* and $P_{004}=1.086$ for sample *B*, in good agreement with the present XSW measurements.

For sample *C*, the geometrical factor a_{004} is expected to be smaller than unity due to the multiple In positions. If we model the buried layer as one full ML of InAs plus 0.1 ML of InAs in the second layer, the In distribution could be characterized by two distinct lattice positions z_1 and z_2, and the corresponding (004) Fourier component would become $CD_{004}[0.91\exp(2\pi i z_1)+0.09\exp(2\pi i z_2)]$. The vertical strain of 7.3% for InAs on GaAs(001) suggests that $z_1=0.15$ and $z_2=0.45$. We can therefore express the coherent fraction to be $f_{004}=0.76C$, which estimates $C=0.88$ as compared with the measured $f_{004}=0.67$. The coherent position calculated from this simple model is 1.165, in good agreement with the experiment as well.

On a microscopic scale, Woicik *et al.* recently reported bond-length calculations based on a random-cluster approximation for tetragonally distorted $\mathrm{In}_x\mathrm{Ga}_{1-x}\mathrm{As}$ layers on GaAs(001), GaAs(111) (Ref. 18), and InP(001).[19] Excellent agreement of these calculations with measurements has been demonstrated by extended x-ray absorption fine structure[19,20] (EXAFS) and diffraction anomalous fine structure.[21] Their (001) calculations showed that the In-As bond length in the strained film depended very weakly on the In concentration *x*, in contrast to the monotonous increase of the In height measured in our present work and predicted by macroscopic elasticity theory. The cluster used in Woicik's calculation, however, is for films much thicker than one ML. If the In-As bond length exhibits the same constancy behavior at the one-ML limit, mechanisms other than bond stretching must exist to account for the variation of the In positions we measured. To understand microscopically how the lattice of a buried single layer responds to a biaxial stress, and to compare it with the macroscopic description of strain effect discussed above, we performed a similar random-cluster calculation for one ML of $\mathrm{In}_x\mathrm{Ga}_{1-x}\mathrm{As}$ buried in GaAs(001). The results of our calculation agree well with the present XSW measurements as well as the previous theoretical predictions[18,22] and experimental observations[9,11,20,21] for the local structures of $\mathrm{In}_x\mathrm{Ga}_{1-x}\mathrm{As}$ strained layers.

Our calculation follows essentially the approach discussed in Ref. 18, which is a simplified version of the quasichemical approximation (QCA) developed by Sher *et al.*[23] Figure 3 shows the 42-atom cluster together with the 44 medium atoms used in the present calculation. The cluster was constructed from a planar core to account for the two-dimensional nature of the buried ML. The 4 cation sites at the center of the cluster are occupied randomly by *j* In atoms and $4-j$ Ga atoms. The 12 anions in the first shell are As atoms. In the second shell, the top and the bottom layers are occupied by 18 Ga atoms, and the middle layer is occupied by $8\,\mathrm{In}_x\mathrm{Ga}_{1-x}$ virtual atoms (each one has the properties averaged over In and Ga based on *x*). Finally, there are 44 As atoms in the third shell. Statistically the QCA method requires the cluster to be independent of the surrounding matrix. To uncouple the cluster from the rest of the lattice, the

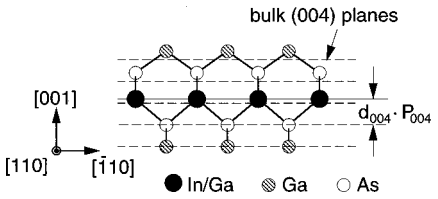

FIG. 2. The [110] projected side view depiction of a pseudomorphically grown 1-ML $\mathrm{In}_x\mathrm{Ga}_{1-x}\mathrm{As}$-buried heterostructure. The dashed lines represent the (004) Ga and As planes of the GaAs substrate, and the solid line indicates the In/Ga position in the buried film with respect to the (004) planes.

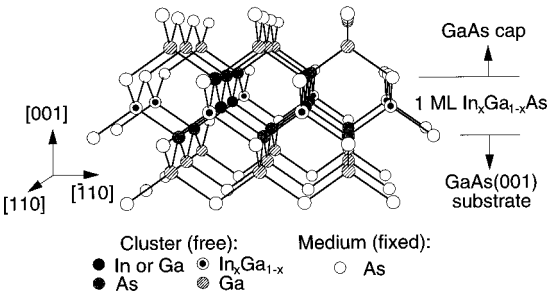

FIG. 3. The 42-atom cluster and the surrounding 46 medium atoms used in the present calculation for 1-ML $\mathrm{In}_x\mathrm{Ga}_{1-x}\mathrm{As}$-buried in GaAs(001). During the energy minimization, only the atoms within the cluster are allowed to relax. The medium atoms are fixed at their tetragonally distorted virtual-crystal sites.

44 third-shell As atoms (or the medium atoms) are fixed at their tetragonally distorted virtual-crystal sites.

For the zinc-blende structure, the short-range interaction between atoms can be described by the Keating valence-force field[24] model, where the total strain energy of the system is expressed as a two-force-constant equation

$$E=\sum_i \frac{3}{8}\frac{\alpha_i}{r_{i,0}^2}(r_i^2-r_{i,0}^2)^2+\sum_i \sum_{j=1}^{3}\sum_{k>j}^{4}\frac{3}{8}\frac{\beta_{ijk}}{r_{ij,0}r_{ik,0}} \times\left(\mathbf{r}_{ij}\cdot\mathbf{r}_{ik}+\frac{r_{ij,0}r_{ik,0}}{3}\right)^2. \quad (5)$$

The first term is the strain energy due to bond stretching, characterized by the two-body radial-force constant α and summed over all the bonds within the cluster. The second term accounts for the strain energy due to bond bending, characterized by the three-body angular-force constant β and summed over all the atoms within the cluster.[25] The **r**'s are the bond vectors between two neighboring atoms and the subscript 0 denotes an unstrained bond length. The energy due to chemical effects was ignored in this calculation.[18] To correct the overestimation of the strain energy caused by fixing the medium atoms in space,[23] we weakened the cluster-medium interaction by setting $\beta=0$ whenever a Ga-As bond between the third shell and a Ga atom in the top or the bottom layers of the second shell was involved in the calculation of the second term in Eq. (5). The third-shell As atoms were allowed to have three-body angular interaction with the cluster only through the 8 In_xGa_{1-x} virtual atoms in the middle layer of the third shell. This is necessary in providing the rigidity against the lateral expansion of the $In_xGa_{1-x}As$ ML.

All the atoms were initially located at their tetragonally coordinated virtual-crystal sites, which have the same in-plane coordinates as the GaAs substrate. The vertical initial position of each atomic layer was determined by minimizing the strain energy per In_xGa_{1-x} atom using Eq. (5) for an artificially constructed monolayer of In_xGa_{1-x} virtual atoms buried in GaAs(001). The 42 atoms within the cluster were then allowed to move until Eq. (5) reached its minimum.[26] For each composition, six different clusters were considered to explore all the possible arrangements for In or Ga to occupy the four cation sites at the center of the clusters. The structural dimensions obtained from the individual clusters were then averaged according to their population, which was determined by the Bernoulli distribution for a given x and the degeneracy of each cluster.

Figures 4, 5, and 6 show the results of the calculation averaged over the six clusters as a functions of the In concentration x. In Fig. 4 we directly related the vertical positions of the atoms in the $In_xGa_{1-x}As$ layer to the nearest (004) As plane extrapolated from the substrate. This was accomplished by assuming that the bottom As layer in Fig. 3 is aligned with a substrate (004) plane. Figure 4(a) shows the calculated In coherent position P_{004} in unit of the GaAs (004) d spacing. The cluster calculation predicts a nearly linear dependence of P_{004} on x, which is basically identical to the trend suggested by the macroscopic theory using Eqs. (1) and (4). In Fig. 4(a), the calculated curve agrees not only with the present XSW data (A and B) but also with the statistically averaged In position (1.157 ± 0.01) of three earlier measurements[9–11] for $x=1.0$ (D).

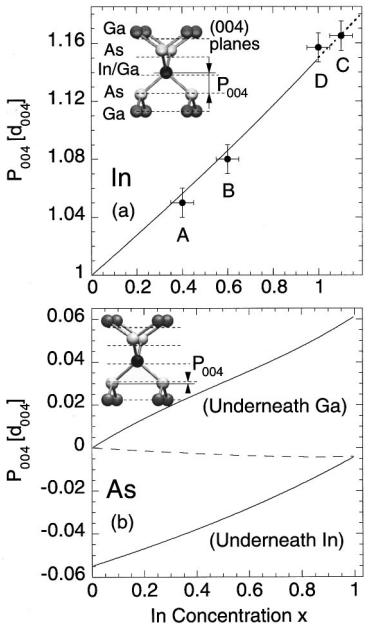

FIG. 4. The calculated vertical positions with respect to the nearest substrate GaAs(004) As plane as a function of the In concentration x for (a) the In atoms in the buried ML and (b) the As atoms right below the In_xGa_{1-x} layer. The measured positions A, B, and C in (a) are from the present XSW experiment for samples A, B, and C, respectively. The data point D is the statistically averaged value of the In P_{004} positions for $x=1.0$ in Refs. 9, 10, and 11. The dashed line in the $x>1.0$ region in (a) is calculated assuming a full ML of InAs in the first layer plus a sub-ML of InAs in the second layer. The dashed line in (b) is the population-weighted average over the two solid lines.

Figure 4(b) shows the (004) positions for the As atoms right below the In_xGa_{1-x} layer that form bonds with an In atom (the lower curve) or a Ga atom (the upper curve). For those As atoms underneath In, the theory suggests a vertical deviation from their bulk positions, which can be as large as -5.5% of the GaAs(004) d spacing at the limit of very dilute In. This is due to the fact that these As atoms are pushed down by the bigger In atoms above, which are held by the surrounding lattice. The lower the In concentration, the more GaAs like the buried monolayer, and therefore the larger this effect. For $x=1.0$, the entire heterolayer is covered by In, and thus the As at the interface are free vertically to resume their bulklike positions.[27] The opposite effect is predicted for the P_{004} of the As underneath Ga.

Figures 5(a) and 5(b) show the change in the second-nearest-neighbor distances along the $[\bar{1}10]$ direction (d_1) and along the [101] direction (d_2), respectively, between the As atoms right below and above the In_xGa_{1-x} layer. The As-In-As case and the As-Ga-As case were considered separately in each figure. The vertical scale has been normalized to the corresponding distance for the GaAs substrate $d_{s0}=a_{s0}/\sqrt{2}=3.997$ Å. At the dilute In limit, the As-In-As separation is about 5.3% larger than d_{s0} for both d_1 and d_2, which is comparable to the lattice mismatch between InAs and GaAs. The similar As-As distance in all directions implies that the InAs tetrahedron remains the threefold symme-

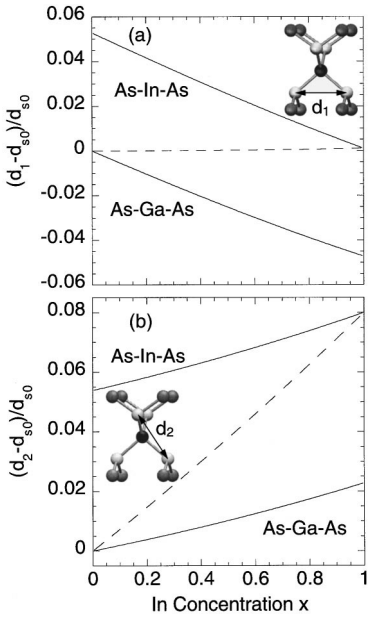

FIG. 5. The calculated compositional dependence of the variation of the second-nearest-neighbor As-As distance for the As atoms right below and above the In_xGa_{1-x} layer. The solid lines are the average of the As-As distances along the $[\bar{1}10]$ and $[110]$ directions (a), and the average over the $[011]$, $[101]$, $[0\bar{1}1]$ and $[\bar{1}01]$ directions (b). In each calculation, those As atoms bonding to In and those to Ga in the buried layer are considered separately. The dashed line in each figure is the population-weighted average over the two solid lines.

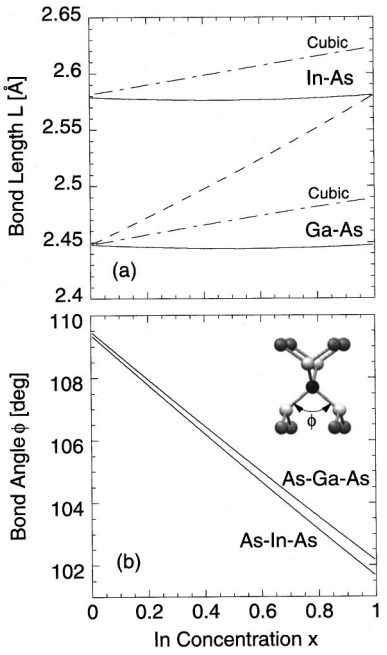

FIG. 6. The calculated (a) In-As and Ga-As bond lengths L and (b) As-In-As and As-Ga-As bond angles ϕ in the $In_xGa_{1-x}As$ ML as functions of the In concentration x (solid lines). The long-dashed lines in (a) are the In-As and the Ga-As bond lengths for cubic $In_xGa_{1-x}As$. The calculation in (b) considers only the bond angle as indicated in the inset. The dashed line in (a) is the population-weighted average over the two solid lines.

try for small x. As x increases, the lateral compression builds up gradually as a result of increasing lattice mismatch and hence causes both the As-In-As and As-Ga-As separations along the $[\bar{1}10]$ directions to decrease. The former finally approaches to d_{s0}, as required by symmetry, and the latter becomes 4.7% smaller than d_{s0} for $x=1.0$ due to the local expansion of the InAs tetrahedrons surrounding each Ga atom. Meanwhile, the vertical expansion of the buried layer leads to larger As-In-As and As-Ga-As distances along the $[101]$ direction towards higher x. Therefore, our calculation renders a split between d_1 and d_2 for both the As-In-As and As-Ga-As distances. The same effect has been measured by polarization-dependent EXAFS of the second-shell distance of Ge for a coherently grown GeSi layer on Si(001).[28]

Figure 6(a) shows the In-As and the Ga-As bond lengths L (solid lines) in the strained $In_xGa_{1-x}As$ monolayer. For comparison, we also plotted the bulk-alloy bond lengths calculated for cubic $In_xGa_{1-x}As$ (long-dashed lines). For the strained bond lengths, our calculation agrees with Woicik's results[18] for a thick $In_xGa_{1-x}As$ film on GaAs(001). Both the In-As and Ga-As bond lengths are essentially constant over the range of $0 \leqslant x \leqslant 1$: the In-As bond stays at about 98% of its natural bond length ($L_{\text{In-As},0}=2.623$ Å) and the Ga-As bond remains nearly unstrained ($L_{\text{Ga-As},0}=2.448$ Å). This tendency is the main cause of the local lattice distortion around In atoms at lower x (and around Ga atoms at higher x) suggested in Figs. 4(b) and 5(a). When compared with the bond lengths in cubic $In_xGa_{1-x}As$, the In-As and Ga-As bonds in a strained ML are equally contracted, as observed and explained by Woicik *et al.*[20,21] for a 213 Å-thick $In_{0.22}Ga_{0.78}As$ on GaAs(001). The contraction of the In-As bond length at the one-ML limit has been measured by Woicik *et al.*[9,11] using EXAFS. They reported an In-As bond length of 2.57 ± 0.02 Å for $x=1.0$, in good agreement with the present calculation. Since the As atoms right below a full ML of In were shown [Figs. 4(b) and 5(a)] to have bulklike positions, we can also estimate the In-As bond length from the XSW-measured In height through $L_{\text{In-As}} = 0.25 a_{s0}\sqrt{P_{004}^2+2}$ for a strained, pure InAs monolayer. Using the statistically averaged value of the In P_{004} positions in Refs. 9, 10, and 11 for $x=1.0$, the above formula renders a bond length $L_{\text{In-As}}=2.582$ Å, consistent with the present calculation and the EXAFS findings. At the limit of very dilute In, the In-As and Ga-As bond lengths in strained and cubic $In_xGa_{1-x}As$ should converge to the same values. Our calculated bond lengths at this limit are therefore supported by the measurements reported by Mikkelsen and Boyce.[29] However, our results do not predict the stretched Ga-As bond length observed by Proietti *et al.*[30,31] in their EXAFS measurements of $In_xGa_{1-x}As$ films on GaAs(001).

Figure 6(b) shows the As-In-As and As-Ga-As bond angles ϕ in the heterolayer as defined in the inset. For the sp^3 hybrid orbitals the natural bond angle is $\phi_0=109.47°$. Our calculation indicates that the As-In-As and As-Ga-As bond angles are close to ϕ_0 for small x. As x increases, the As-In-As as well as the As-Ga-As bond angles decrease due to the in-plane stress. The total bond bending is about 8° for both InAs and GaAs tetrahedrons over the entire compositional range. Notice that this bond-angle adjustment is directly related to the strong x dependence of the As-As distance in Fig. 5 and the (004) In position in Fig. 4(a), but not a result of elongation of In-As or Ga-As bond.

The dashed lines in Figs. 4(b), 5, and 6(a) were obtained by averaging in each figure the two solid lines after they were properly weighted with either the In or the Ga population in the buried layer. They represent the structural dimensions that would be predicted by the virtual-crystal model,[19] which disregards the distinction between In and Ga and treats each atom in the buried layer as a virtual In_xGa_{1-x} atom. The dashed lines in Figs. 4(b) and 5(a) imply that the average position of the As atoms at the bottom of the $GaAs/In_xGa_{1-x}$ interface is already bulklike. Therefore, macroscopically the regions beyond the first-nearest neighbor of In_xGa_{1-x} are essentially unstrained. This justifies our earlier assumption in defining the boundary of the strained region for applying the macroscopic elasticity theory to a buried ML.

In contrast to the linearity of the bulk-alloy lattice constants predicted by Vegard's law, the calculated In height, bond lengths and As-As second-nearest-neighbor distances (d_1 and d_2) exhibit nonlinear behaviors under biaxial stress. This has an origin in the fact that the perpendicular strain (or the lattice constant c) of a tetragonally distorted film is not a linear function of the film composition [Eq. (1)]. In Fig. 6(a), for example, the effect of the substrate constraint against the film lateral expansion causes the In-As and Ga-As bond lengths to deviate from following the straight lines for the bulk alloy, and the nonlinear nature of the vertical expansion of the film leads to the slight bowing of the theoretically evaluated bond length curves.

Based on our XSW measurements and cluster calculation, we now have a microscopic description of the effect of strain on a ML-thick film. At very low-In concentration, the stress around each In atom remains isotropic. Thus, the As-In-As bond angle stays close to its natural value. The incorporation of In atoms causes primarily the four first-nearest-neighbor As atoms of each In to be pushed away from their bulk positions. As the In concentration rises, the In_xGa_{1-x} layer begins to form and the stress becomes more lateral. This increasing biaxial compression bends the As-In-As and As-Ga-As bond angles, but the more InAs-like environment allows the four nearest-neighbor As atoms of each In to move back to their tetragonally coordinated virtual-crystal positions. As a result, the buried layer expands vertically. Over the entire compositional range, the In-As and Ga-As bonds in the buried layer are equally contracted in such a way that their bond lengths remain constant. Therefore, our calculation suggests that the bond-length strain in a one-ML $In_xGa_{1-x}As$ film is accommodated through the combination of (a) the As-In-As and As-Ga-As bond bending, (b) the equal contraction of In-As and Ga-As bond lengths, and (c) the local lattice distortion at the $GaAs/In_xGa_{1-x}As$ interfaces. Factors (a) and (c) are also responsible for the variation of the In height. Factors (a) and (b) are expected to have larger effect for higher In concentrations, while (c) should become more pronounced near the dilute In or Ga limit. Since our single-ML calculation and the result in Ref. 18 for a thick overlayer predict the same compositional dependence for In-As and Ga-As bond lengths, our above conclusion should also be valid for the case of a thick $In_xGa_{1-x}As$ layer grown on GaAs(001).

The success of the macroscopic continuum elasticity theory in calculating the position of one ML of In_xGa_{1-x} buried in GaAs(001) can be further appreciated if we consider applying the same theory to a strained film grown along the [111] direction. The complication of the (111) case originates from the fact that the four different directions that the tetrahedral bonds point to in a [111]-oriented film are not all equivalent with respect to the lateral stress. The bond along the [111] direction is expected to be less strained than the bonds parallel to the $[\bar{1}11]$, $[1\bar{1}1]$, and $[11\bar{1}]$ directions.[18] Therefore, the contraction or expansion of the lattice may not be uniform in the [111] direction. We are currently investigating the (111) case and the related issues will be discussed in a separate report.

In summary, x-ray standing wave measurements were carried out to study the strain in pseudobinary $In_xGa_{1-x}As$ alloys buried in GaAs(001) at the one monolayer limit. The measured In positions along the (001) direction were found in good agreement with the values predicted by macroscopic continuum elasticity theory. A more microscopic description of the strain effect was obtained by performing a random-cluster calculation using the Keating valence-force field. With a cluster specially constructed for a buried, one ML-thick film, our calculation shows a weak compositional dependence of the In-As and Ga-As bond lengths. This is similar to the results from an earlier calculation for a thick $In_xGa_{1-x}As$ film on GaAs(001).[18] In addition, the calculated As-In-As bond angles and the positions of the first-nearest-neighbor As atoms suggest that the strain in the buried monolayer is accommodated through the combination of the As-In-As and As-Ga-As bond bending, the equal contraction of the In-As and Ga-As bond lengths, and the local lattice distortion at the $GaAs/In_xGa_{1-x}$ interfaces. The bond bending and the local lattice distortion are also found to be the cause of the vertical expansion we measured in the strained layers.

This work was supported by the U.S. Department of Energy under Contract No. W-31-109-ENG-38 to Argonne National Laboratory, Contract No. DE-AC02-76CH00016 to the National Synchrotron Light Source at Brookhaven National Laboratory, and by the National Science Foundation under Contracts No. DMR-9632593 to M.J.B. and No. DMR-9632472 to the MRC at Northwestern University.

[1] For example, F. Martelli, A. Polimeni, A. Patane, M. Capizzi, P. Borri, M. Gurioli, M. Colocci, A. Bosacchi, and S. Franchi, Phys. Rev. B **53**, 7421 (1996); W. E. Hoke, P. S. Lyman, J. J. Mosca, H. T. Hendriks, A. Torabi, W. A. Bonner, B. Lent, L.-J. Chou, and K. C. Hsieh, J. Appl. Phys. **81**, 968 (1997).

[2] S. T. Chou, K. Y. Cheng, L. J. Chou, and K. C. Hsieh, Appl. Phys. Lett. **66**, 2220 (1995).

[3] T. Mattila, L. Bellaiche, L.-W. Wang, and A. Zunger, Appl. Phys. Lett. **72**, 2144 (1998).

[4] For example, S. Picozzi, A. Continenza, and A. J. Freeman, Phys. Rev. B **52**, 5247 (1995).

[5] *Semiconductors: Group IV Elements and III-V Compounds*, edited by O. Madelung (Springer-Verlag, Berlin, 1991).

[6] O. Brandt, K. Ploog, R. Bierwolf, and M. Hohenstein, Phys. Rev.

Lett. **68**, 1339 (1992).
[7] C. Giannini, L. Tapfer, S. Lagomarsino, J. C. Boulliard, A. Taccoen, B. Capelle, M. Ilg, O. Brandt, and K. H. Ploog, Phys. Rev. B **48**, 11 496 (1993).
[8] J. E. Bernard and A. Zunger, Appl. Phys. Lett. **65**, 165 (1994).
[9] J. C. Woicik, J. G. Pelligrino, S. H. Southworth, P. S. Shaw, B. A. Karlin, and C. E. Bouldin, Phys. Rev. B **52**, R2281 (1995).
[10] T.-L. Lee, Y. Qian, P. F. Lyman, J. C. Woicik, J. G. Pellegrino, and M. J. Bedzyk, Physica B **221**, 437 (1996).
[11] J. C. Woicik, K. E. Miyano, J. G. Pellegrino, P. S. Shaw, S. H. Southworth, and B. A. Karlin, Appl. Phys. Lett. **68**, 3010 (1996).
[12] J. G. C. Labanda, S. A. Barnett, and L. Hultman, Appl. Phys. Lett. **66**, 3114 (1995).
[13] Y. Qian, N. Sturchio, R. Chiarello, P. F. Lyman, T.-L. Lee, and M. J. Bedzyk, Science **265**, 1555 (1994).
[14] This energy scan is equivalent to scanning the angle of the sample substrate about the Bragg angle, and the abscissas of the XSW data will be expressed as angular deflections for convenience.
[15] For a review of dynamical diffraction theory, see B. W. Batterman and H. Cole, Rev. Mod. Phys. **36**, 681 (1964).
[16] M. J. Bedzyk and G. Materlik, Phys. Rev. B **31**, 4110 (1985); M. J. Bedzyk and G. Materlik, *ibid.* **31**, 4110 (1985).
[17] $D_{004}=\exp(-B/2d_{004}^2)$, where $B=0.59\ \text{Å}^2$ is from T. Matsushita and H. Hayashi, Phys. Status Solidi A **41**, 139 (1997); *International Tables for X-Ray Crystallography*, edited by C. H. MacGillavry *et al.* (Kynoch, Birmingham, England, 1962), Vol. III.
[18] J. C. Woicik, Phys. Rev. B **57**, 6266 (1998).
[19] J. C. Woicik, J. A. Gupta, S. P. Watkins, and E. D. Crozier, Appl. Phys. Lett. **73**, 1269 (1998).
[20] J. C. Woicik, J. G. Pellegrino, B. Steiner, K. E. Miyano, S. G. Bompadre, L. B. Sorensen, T.-L. Lee, and S. Khalid, Phys. Rev. Lett. **79**, 5026 (1997).
[21] J. C. Woicik, J. O. Cross, C. E. Bouldin, B. Ravel, J. G. Pellegrino, B. Steiner, S. G. Bompadre, L. B. Sorensen, K. E. Miyano, and J. P. Kirkland, Phys. Rev. B **58**, R4215 (1998).
[22] A. Amore Bonapasta and G. Scavia, Phys. Rev. B **50**, 2671 (1994).
[23] A. Sher, Mark van Schilfgaarde, An-Ban Chen, and W. Chen, Phys. Rev. B **36**, 4279 (1987).
[24] P. N. Keating, Phys. Rev. **145**, 637 (1966).
[25] The values of the constants α and β for InAs and GaAs used in this calculation were taken from R. M. Martin, Phys. Rev. B **1**, 4005 (1970).
[26] The energy minimization process followed the conjugate gradient method described in W. H. Press, S. A. Teukolsky, W. T. Vetterling, and B. P. Flannery, *Numerical Recipes in Fortran*, 2nd ed. (Cambridge University Press, Cambridge, England, 1994).
[27] For $x=1.0$, the vertical position of the As underneath In is about 0.4% of d_{004} lower than the bulk As position. This can be understood from the fact that, under the same strain condition, the Ga-As bond length is expected to be shorter if the As atom bonds to Ga and In atoms simultaneously (see discussion in Ref. 18).
[28] J. C. Woicik, C. E. Bouldin, K. E. Miyano, and C. A. King, Phys. Rev. B **55**, 15 386 (1997).
[29] J. C. Mikkelsen, Jr. and J. B. Boyce, Phys. Rev. Lett. **49**, 1412 (1982); Phys. Rev. B **28**, 7130 (1983).
[30] M. G. Proietti, F. Martelli, S. Turchini, L. Alagna, M. R. Bruni, T. Prosperi, M. G. Simeone, and J. Garcia, J. Cryst. Growth **127**, 592 (1993).
[31] M. G. Proietti, S. Turchini, J. Garcia, G. Lamble, F. Martelli, and T. Prosperi, J. Appl. Phys. **78**, 6574 (1995).